Experimental Demonstration of mm-Wave 5G NR Photonic Beamforming Based on ORRs and Multi-Core Fiber

Maria Morant, *Member, IEEE,* Ailee Trinidad, *Student Member, IEEE,* Eduward Tangdiongga, *Member, IEEE,* Ton Koonen, *Fellow, IEEE*, and Roberto Llorente, *Member, IEEE*

Abstract— A photonic beamformer system designed for next-generation 5G new radio (5G NR) operating in the millimeter-wave band is proposed and demonstrated experimentally, including its performance characterization. The photonic beamforming device is based on optical ring resonators (ORRs) implemented on Si_3N_4 and assisted with multi-core fiber (MCF) to feed the different antenna elements (AEs). Fast-switching configuration of the ORRs is performed changing the operating wavelength, as tuning the wavelength modifies the coupling coefficient of the rings and, consequently, the induced time delay. Multi-beam operation is evaluated at 17.6 GHz and 26 GHz radio keeping the ORRs' configuration. The beamforming performance is evaluated using single-carrier signals with up to 128QAM modulation over up to 4.2 GHz electrical bandwidth. The experimental beamforming system with 2 AEs provides up to 21 Gbps per user, while the beamforming system with 4 AEs provides up to 16.8 Gbps per user. Wireless transmission confirms that changing the wavelength from 1545.200 to 1545.195 nm modifies the beam steering from 11.3° to 23° with 26 GHz signals (5G NR pioneer band in Europe).

Index Terms— 5G new-radio, beam steering, multi-core fiber, optical ring resonators, radio-over-fiber

I. INTRODUCTION

BEAMFORMING in cellular base stations is the most efficient approach to reduce the interference from nearby users and to compensate atmospheric attenuation losses. This is of special importance when using high-frequency bands with very large bandwidths, as the bands proposed for next-generation 5G New-Radio specification (5G NR) for cellular networks [1]. 5G NR targets to provide ultra-high capacity with very different user profiles, from low-latency
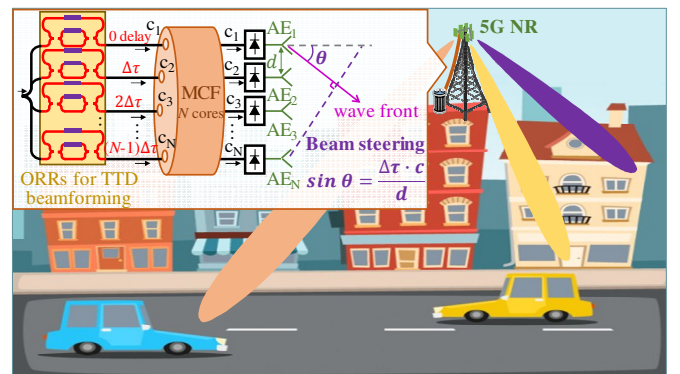
Fig. 1. 5G NR scenario with beamforming provided by MCF and ORRs

applications as Internet-of-Things (IoT) or connected vehicles to massively high-bitrate applications as 8K video or high-definition virtual reality applications [2].

5G NR is focusing on high-frequency bands above 24 GHz spectral range (commonly known as millimeter-wave or mm-wave in 5G NR communications [3]). In 5G NR cellular radio, atmospheric attenuation is the most important transmission impairment to deal with. A ten-fold increase in the carrier frequency of mm-wave signals is translated to an order-of-magnitude increase in free-space transmission loss [4]. For this reason, one of the key enablers for 5G relies on the beam-steering capabilities to overcome signal blocking [3]. This is further facilitated because, as the carrier frequency increases, the antenna elements (AEs) become smaller, thus larger number of AEs per antenna site are feasible [5]. A phase array antenna (PAA) consists of an array of multiple AEs and a beamformer that feeds each AE with different delays. PAA's main advantages include beam shaping and beam steering, interference nulling and the capability to generate multiple antenna beams [6]. PAAs provide agile beam steering and relatively low maintenance costs compared with mechanically steered antennas [7]. Beamforming can be implemented analogically (with opto-electronic devices as proposed in this work) or digitally (e.g. using digital multiple-input multiple output (MIMO) processing [8]). The first implementations for generating optical true-time delay (TTD) were based on free-space optics [9]. In order to be able to change the transmission/reception angle of the PAA, the induced time delays should be tunable [7]. To date, different optical implementations have been reported, including beamformers based on optical phase shifters [10], switchable fiber optic

delay matrices [11] or combining dispersive optical devices like high-dispersion fiber [12] or fiber-Bragg gratings [13]. In this work, we evaluate the performance of an opto-electronic beamforming system suitable for 5G NR using a photonic TTD device based on optical ring resonators (ORRs) assisted with multi-core fiber (MCF). The proposed photonic TTD integrated circuit was initially evaluated for two-dimensional radio beamforming for satellite communications in [14]. This photonic TTD device has the advantage of wide bandwidth (BW) compared with traditional electronic beamformers that have an intrinsic narrowband response and deform the beam when operating with broadband signals [15]. The proposed TTD device comprises several ORRs in cascade with optical side band filters (OSBFs) that provide a linear phase shift over a large bandwidth (i.e. 0.48 nm free spectral range) with reduced weight and size (i.e. 16×16 mm^2 [14]) and immunity to electromagnetic interference. In order to further reduce the size and complexity of the beamforming system, the use of MCF to feed the different AEs of the PAA is proposed in this work, which also ensures that all the optical paths of the beamforming system have the same length. With a centralized control of the ORRs, we can configure the different delays to be 0, $\Delta\tau$, $2\Delta\tau$… $(N-1)\Delta\tau$, considering an array antenna with N elements and a MCF with N cores as depicted in Fig. 1. Using MCF enables centralizing 5G advanced functionalities like beamforming [16] and MIMO [17] at the central office, thus simplifying and reducing the cost and power consumption of the remote antenna units. 5G base stations are expected to comprise large numbers of AEs to link multiple user terminals while using the same frequency resources. In this way, opto-electronic beamforming can be implemented altogether with massive MIMO signal-processing algorithms to achieve optimum transmission performance for each user [18]. Deploying more antenna elements in massive MIMO, the resulting beam also gets narrower [19], and it becomes possible to steer the transmission towards a particular user (or set of users) to improve the cellular coverage [19]. As fully digital beamforming is expected to handle multiple data streams from a single array [20], the experimental demonstration evaluates the performance of multiple beams in the Ka-band.

3GPP Technical Specification Groups have just presented the first specifications of 5G NR in Release-15 in September 2018 [1], while 5G phase 2 (Release-16) should be completed by December 2019 [21]. In the United States, the Federal Communications Commission (FCC) made available 11 GHz of spectrum at 28 GHz, 37-40 GHz and 64-71 GHz for 5G mm-wave applications. In China, Japan and South Korea, early 5G focuses on 28 GHz. In Europe, the 26 GHz band is being prioritized as the first high frequency band for 5G [3]. In particular, 3GPP band n258 refers to the range between 24.25 and 27.5 GHz (covering 3.25 GHz of spectrum). In 2016, SK Telecom and Ericsson conducted the first multi-vehicular 5G trials with BMW demonstrating a Ka-band 5G system with beam tracking and mobility [22]. In May 2018, DoCoMo (who will show its 5G technology for the Olympics in 2020) demonstrated a 1.1 Gbps ultrahigh-speed data transmission via

downlink to a 5G mobile station [23][24]. The trend in this band is to use 4-channel transmit/receive chips to control packs of 4 antennas [5][21]. In this work, we evaluate beamforming systems with 4 AEs employing a commercial 4-core fiber (4CF) and a photonic TTD device based on ORRs. The proposed system can be scaled up employing high-density MCF media. Currently, there are also homogeneous 7-core and 19-core MCFs commercially available with hexagonal close packing of cores [25]. MCF achieved a core count up to 32 with low crosstalk of −40 dB per 100 km [26] that could be used to feed the 32-element 5G array antenna proposed in [5]. In DoCoMo trial, the 5G base stations used a massive-element antenna with 96 elements (and up to two beams)[24] that could be fed with three MCFs of 32 cores each (instead of using 96 single-core fibers).

This paper is structured as follows: In Section II, the TTD device based on ORRs combined with MCF is depicted. The increment delay ($\Delta\tau$) induced by each ORRs is characterized experimentally and the beam-steering angle in a beamforming system with 4 AEs is analyzed by simulation. Multi-beam operation at 17.6 and 26 GHz radio covering bandwidths up to 4.2 GHz with quadrature amplitude modulation (QAM) orders up to 128QAM is evaluated experimentally using a MCF to feed each AE. Next, in Section III, the performance of a 2×1 beamforming system is evaluated experimentally including the wireless link at 26 GHz. Finally, in Section IV, the main conclusions of this work are highlighted.

II. BEAMFORMING PERFORMANCE EVALUATION

Fig. 2 shows the experimental setup developed to evaluate a beamforming system with 4 AEs that are fed with a 4CF with different delays induced by four ORRs. Single-carrier data signals are defined with up to 128QAM over 1.5, 2, 3.25 and 4.2 GHz BW using an arbitrary waveform generator (Tektronix AWG7122B) centered at f_c=4.2 GHz. This signal is upconverted with a local oscillator (LO) at f_{LO}=21.8 GHz. Multi-beam operation is evaluated measuring the performance of both electrical bands in the upconverted signal located at $f_{LO}+f_c$=26 GHz (user #A) and $f_{LO}-f_c$=17.6 GHz (user #B). In a real deployment, different 5G transmitters operating at different frequency bands would be used. The electrical signal is modulated with a 20-GHz BW Mach-Zehnder modulator (MZM) over an optical carrier generated with a distributed feedback (DFB) laser in the 1545 nm wavelength range. Optical single side band (SSB) operation is ensured using an optical filter (OF) with 1.2 nm bandwidth (Santec OTF-950). The filtered signal is amplified with an Erbium doped fiber amplifier (EDFA) and divided into four optical paths to obtain a beamformer to feed 4 AEs. At this point, the TTD device is configured to provide different delays to each path, i.e. 0, $\Delta\tau$, $2\Delta\tau$ and $3\Delta\tau$. The proposed TTD device is based on thermo-optic phase shifters in 2-port ORRs fabricated on Silicon Nitride (Si$_3$N$_4$) [14]. Each ORR has two heaters: one for tuning the resonance wavelength, and another for tuning the coupling coefficient (and, consequently, the induced delay). The fabricated chip also includes OSBFs with 0.48 nm free spectral range to operate with carrier suppressed single side band (CS-SSB) as depicted in [14].
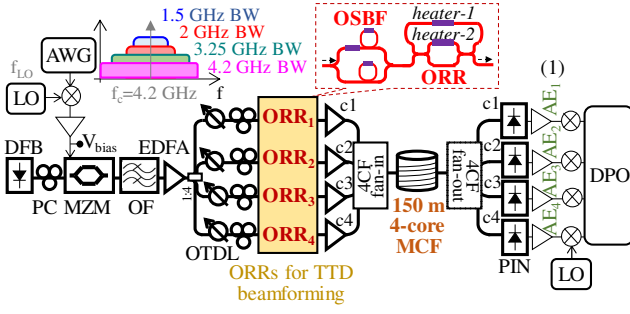
Fig. 2. Experimental setup for the evaluation of a beamforming system to feed 4 AEs employing 4 ORRs and a 4-core fiber
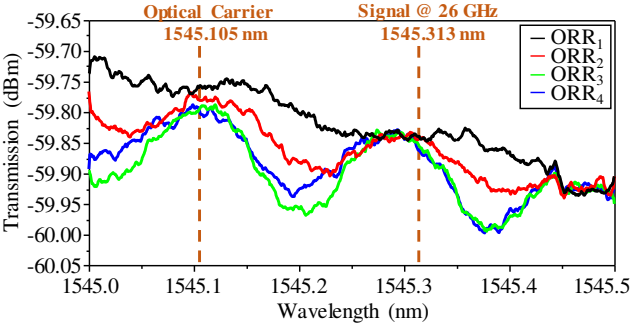

Fig. 3. Optical transmission response of the ORRs in the 1545 nm wavelength range. Vertical dashed lines mark an example of the location of the initial optical carrier at 1545.105 nm and the resulting signal at 26 GHz
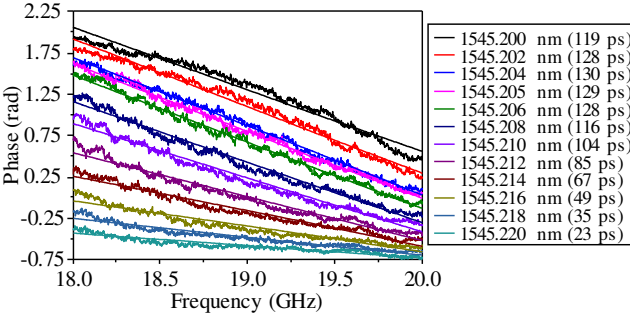

Fig. 4. Example of obtained phase (in radians) measured in the 18-20 GHz radio frequency band for different wavelengths

Fig. 3 shows the optical transmission response of the ORRs in the 1545 nm wavelength range. As an example, the location of an optical carrier at 1545.105 nm and the correspondent signal data at 26 GHz, i.e. 1545.313 nm, are marked with vertical lines in Fig. 3.

The voltages applied to the heaters for the OSBFs and ORRs are configured from a central computer. In order to ensure that the delay between the paths is produced by the TTD chip, the lengths of the optical paths must be the same. Due to the length difference between the single-core fiber pigtails employed in the setup, optical tapped-delay-lines (OTDLs) are included to set the delay difference between the four paths to ~0 ps when the ORRs are off. Once the initial delay between the optical paths is adjusted, the OTDLs' configuration remains constant for all the measurements, only modifying the delay by tuning the voltage applied to the ORRs' heaters. Since one 5G cell may serve hundreds of users, the beam direction may change several times per millisecond [19].
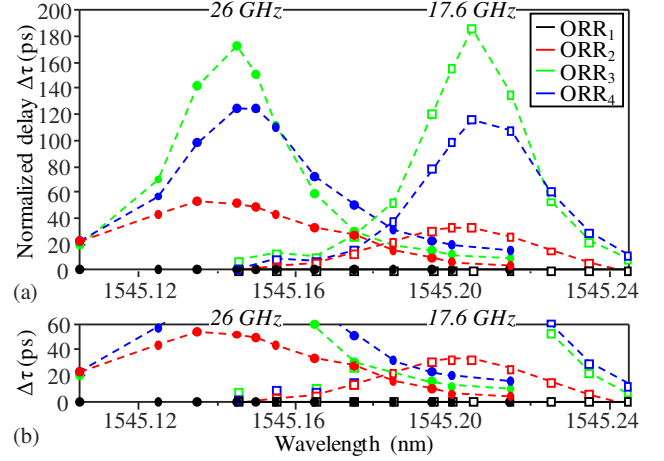

Fig. 5. (a) Normalized increment delay induced by each ORR measured from 1545.105 nm to 1545.245 nm wavelength range for 26 GHz (filled symbols) and 17.6 GHz radio signals (blank symbols) (b) zoom for delays $\Delta\tau > 60$ ps suitable for beamformers with 4 AEs

TABLE I
DELAY INCREMENT BETWEEN AES INDUCED BY TTD ORRS CHIP AND
RESULTING BEAM-STEERING ANGLE θ FOR EACH WAVELENGTH

Frequency	λ_{ORR} (nm)	$\Delta\tau$ (ps) per AE	Angle θ
26 GHz	-	19.23 ps	90° (max)
26 GHz	1545.185 nm	13.83 ps	46°
26 GHz	1545.195 nm	7.51 ps	23°
26 GHz	1545.200 nm	3.77 ps	11.3°
26 GHz	**1545.215 nm**	**−7.7 ps**	**−23.5°**
17.6 GHz	-	28.41 ps	90° (max)
17.6 GHz	**1545.215 nm**	**27.96 ps**	**80°**
17.6 GHz	1545.175 nm	7.93 ps	16.6°
17.6 GHz	1545.165 nm	4.9 ps	10°

In the proposed system, the beam steering can be modified by tuning the ORRs' heaters configuration (slow switching), or by keeping the heaters configuration and tuning the optical wavelength (fast switching). The delay induced at each AE is measured keeping the ORRs' heaters configuration and changing the wavelength of the DFB laser. The delay induced by each ORR is calculated from the unwrapped phase measured with a vector network analyzer (VNA). Fig. 4 represents the phase measured with a VNA sweeping the frequency range between 18 and 20 GHz for different wavelengths in the 1545 nm range. From the measured phase (in radians) the induced delay is obtained according to:

$$\sin\theta = \frac{\Delta\phi \cdot \lambda}{2\pi d} = \frac{\Delta\tau \cdot c}{d} \qquad (1)$$

Fig. 5 shows the normalized increment delay ($\Delta\tau$) obtained with 4 ORRs at different optical wavelengths and radio frequencies. The delays induced by each ORR reported in Fig. 5 were obtained from the unwrapped phase measurements configuring the VNA at 17.6 GHz and 26 GHz, respectively, and changing the laser wavelength. The delay of the signal at core 1 (corresponding to ORR₁ and to feed AE₁) is considered as reference (zero delay) to calculate the delay increment $\Delta\tau$ for the other paths. It can be observed in Fig. 5(a) that a delay

increment larger than $\Delta\tau > 180$ ps can be obtained with the proper thermo-optic configuration of the ORRs. Theoretically, with this increment delay between paths, operating with 26 GHz signals, up to 10 AEs could be fed providing a maximum delay (for 90º beam-steering) of $9\Delta\tau(max) \approx 173$ ps.

The experimental evaluation focuses on a beamformer with four AEs following the 5G trend of using 4-channel transmit/receive chips [5][21]. For 26 GHz signals, a beamformer with 4 AEs requires maximum a delay increment of $3\Delta\tau(max) < 57.7$ ps to not exceed a 90° angle. In Fig. 5(b) a zoom for delay increments up to 60 ps is included. The proposed TTD device could be used for PAAs with more AEs. The current TTD chip includes 16 optical paths and its modular and compact size enables the integration of several chips on the same beamforming platform if needed. Table I summarizes the beam steering angle θ obtained with equation (1) for the increment delay $\Delta\tau$ induced by TTD beamformer for different wavelengths at 26 GHz and 17.6 GHz radio.

The radiated beampattern strongly depends on the antenna configuration, as it can be observed in the simulation results obtained in Fig. 6. Electronic system-level (ESL) design software SystemVue was used to evaluate different antenna configurations comprising 4 AEs arranged in a linear array and in a 2×2 matrix, with each AE separated by half wavelength. The simulation study implements an isotropic pattern radiating in the upper hemisphere. In order to validate the resulting beam steering angles reported in Table I, a 2×2 beamforming system is studied by simulation including the delay increments measured experimentally for signals at 26 GHz and 17.6 GHz. The resulting beam steering angles can be observed in the polar diagram of the beam (phy cut) included in Fig. 7, confirming the theoretical values of Table I.

The experimental study focusses on the quality evaluation of the data signals for different electrical bandwidths in order to test the response of the TTD device assisted with MCF for the provision of 5G signals. In the experimental setup depicted in Fig. 2, polarization controllers (PC) are used at the input of the TTD chip to set the correct polarization of the light. The signals coming out the TTD chip are injected in each core of a 4CF employing 3D fan-in/fan-outs [17].

Fig. 7. Simulated polar diagram in the phy cut of a beamforming system with 4 AEs in 2×2 configuration at (a) 26 GHz and (b) 17.6 GHz for the time delay increments $\Delta\tau$ included in Table I

The experimental evaluation is performed over 150 m of a 4CF –Fibercore SM-4C1500(8.0/125)– and direct PIN photodetection is implemented. The received signals are downconverted and analyzed with an oscilloscope (Tektronix DPO 72304DX) and the error vector magnitude (EVM) is measured with SignalVu analysis software. As 5G NR signal quality requirements have not been defined yet, we consider as reference the theoretical EVM threshold to obtain a bit error rate (BER) of BER$=3.8\cdot10^{-3}$ for error free transmission with 7% redundancy hard-decision forward error correction (HD-FEC) [27]. Fig. 8 shows the measured root mean square (rms) EVM for 26 GHz signals vs. the measured delay for different wavelengths in the 1545 nm range and different voltages applied to the ORRs. Fig. 8(a) shows the performance of the signals going through ORR$_1$ and core 1 to feed the AE$_1$. This delay is considered as reference for the calculation of the delay increment $\Delta\tau$ reported in Fig. 5. It can be observed in Fig. 8(a) that for a low voltage applied in ORR$_1$, a flat delay response is obtained ($\Delta\tau \approx 0$ ps) and the resulting EVM performance is also flat.
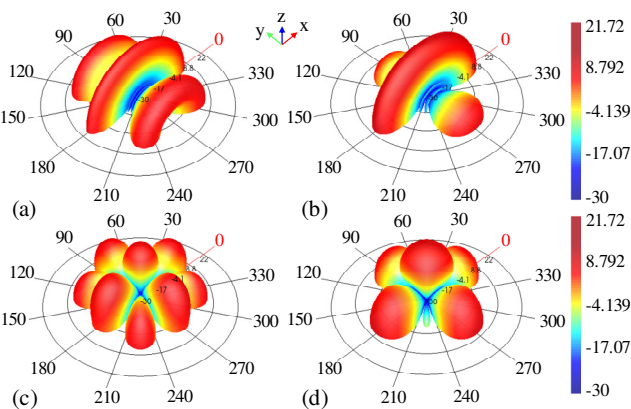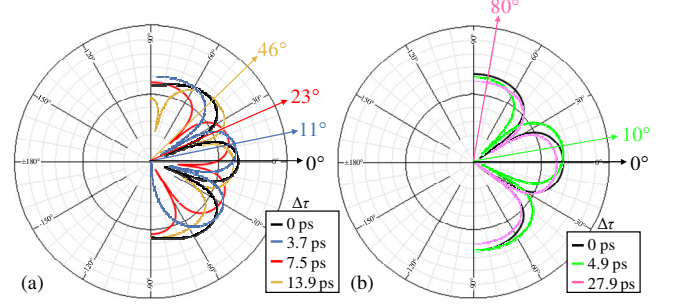

Fig. 6. Beampattern simulation for the same signal input (0 ps delay) considering 4 AEs in: (a) linear array at 26 GHz, (b) linear array at 17.6 GHz, (c) 2×2 matrix at 26 GHz and (d) 2×2 matrix at 17.6 GHz
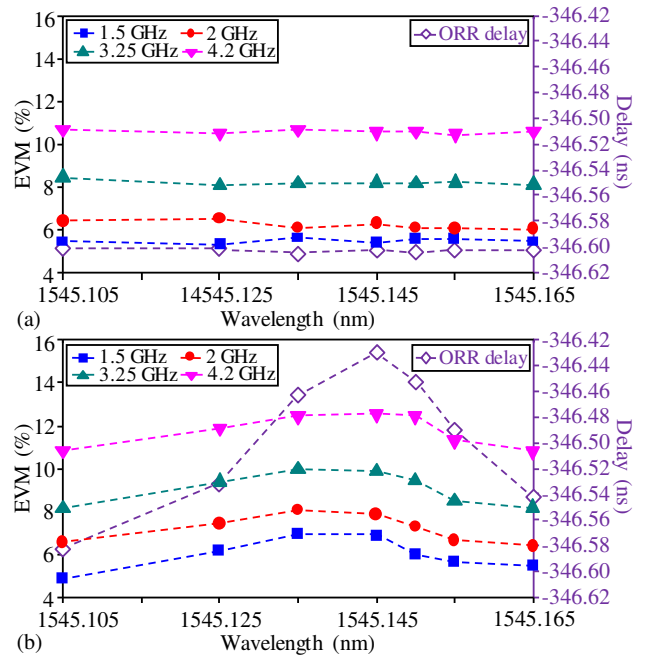

Fig. 8. Measured rms EVM for single-carrier 16QAM signals at 26 GHz with different BWs vs. delay at each wavelength in the 1545 nm range measured for: (a) ORR$_1$ with minimum delay (AE reference, low voltage applied) and (b) ORR$_3$ with higher delay configuration (higher voltage applied)
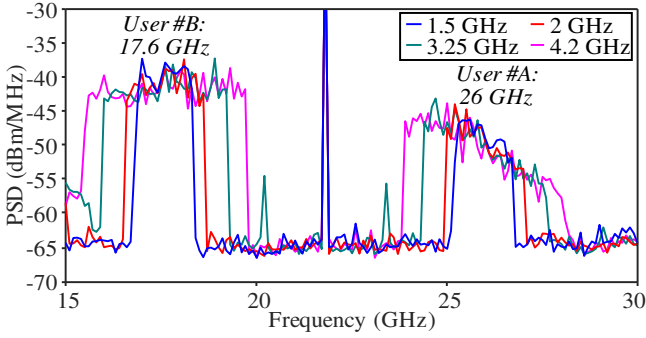
Fig. 9. Measured electrical spectrum at point (1) in Fig. 2 for different BWs

Fig. 8(b) evaluates the performance of ORR₃ with higher voltage applied, where it can be observed that for delay increments higher than $\Delta\tau > 60$ ps in the frequency range around 1545.145 nm, the EVM is slightly worse than for smaller delays. However, this variation never exceeds a 1% EVM increment.

Fig. 9 shows the received power spectral density (PSD) for single-carrier signals with 1.5 GHz to 4.2 GHz BWs measured at point (1) of the experimental setup of Fig. 2 for user #A signals using 26 GHz and user #B at 17.6 GHz. The proposed system can operate with other frequencies with prior characterization of the induced delay. We can observe in Fig. 9 that the high-frequency signals at 26 GHz are affected by the frequency response of the electro-optical devices (20-GHz BW at –3 dB). This affects the EVM performance of user #A at 26 GHz, especially with 3.25 GHz and 4.2 GHz BW signals. However, in all cases, the resulting EVM meets the error-free recommendation of 17.4% for 16QAM signals.

Fig. 10 shows the measured rms EVM for single-carrier signals with 1.5 to 4.2 GHz bandwidth centered in 26 GHz employing up to 128QAM for each ORR operating at 1545.195 nm (23° steering). The experimental results point out that the signals whose ORR is configured to induce higher delays have a slightly worse performance (ORR₄) compared with signals with smaller delay (reference signal at ORR₁). Nevertheless, all the signals of the beamformer meet the EVM recommendation for 3.25 GHz bandwidth signals (5G overall spectrum BW in the 26 GHz band [3]) providing 16.25 Gbps with 32QAM. Higher data rates up to 16.8 Gbps can be provided using 4.2 GHz BW signals employing 16QAM. Higher modulation orders up to 128QAM can be achieved with smaller BW signals (1.5 GHz) providing 10.5 Gbps.

Table II summarizes the data rate provided by a beamforming system with 4 AEs for each signal BW reported in Fig. 10, employing the optimum modulation order to meet the EVM recommendation for all ORRs and operating at 1545.195 nm with a resulting beam steering of 23° at 26 GHz.

TABLE II
PROVIDED DATA RATE FOR EACH 5G SIGNAL BANDWIDTH USING THE OPTIMUM MODULATION ORDER IN A BEAMFORMING SYSTEM WITH 4 AES

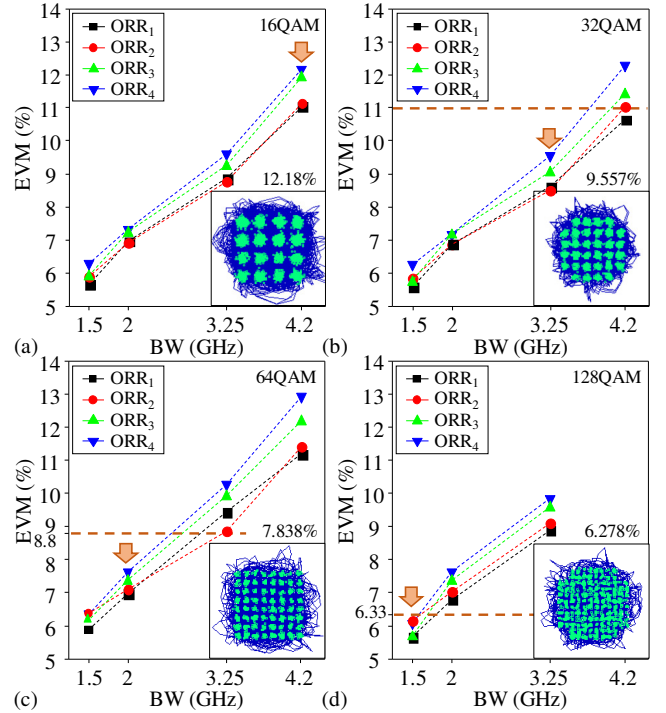| Electrical bandwidth (BW)	Optimum modulation order	Provided data rate
1.5 GHz	128QAM	10.5 Gbps
2 GHz	64QAM	12 Gbps
3.25 GHz	32QAM	16.25 Gbps
4.2 GHz	16QAM	16.8 Gbps

Fig. 10. Measured rms EVM vs. signal bandwidth for all ORRs in a 26 GHz beamformer comprising 4 AEs at 1545.195 nm wavelength (23° steering) using: (a) 16QAM, (b) 32QAM, (c) 64QAM and (d) 128QAM. Horizontal dashed lines indicate the recommended EVM for error-free transmission with BER=3.8·10⁻³. Inset constellations for each modulation order measured for ORR₄ at the highest BW meeting the recommendation (marked with arrows)

III. OPTICAL PERFORMANCE AND WIRELESS BEAM STEERING

Fig. 11 shows the experimental setup employed for the experimental evaluation of a 2×1 beamforming system employing the TTD chip based on ORRs and MCF to feed the AEs of an arrayed antenna. As included in Table I and can be observed in Fig. 12, for the same wavelength at 1545.215 nm, the induced delay at 26 GHz is $\Delta\tau = -7.7$ ps which turns into a $\theta_A = -23.5°$ beam steering for user #A, while at 17.6 GHz the induced delay of $\Delta\tau = 27.96$ ps locates the beam at $\theta_B = 80°$ for user #B. This confirms that the proposed system supports simultaneous users with multiple beams at 26 GHz and 17.6 GHz with $\theta_B - \theta_A = 103.5°$ beam separation.

Fig. 13 shows the measured EVM for single-carrier signals with 1.5 to 4.2 GHz bandwidth in both 26 GHz and 17.6 GHz frequencies in the 2×1 beamforming system operating at 1545.215 nm. Table III summarizes the data rate provided by the 2×1 beamforming system for each BW in a multi-beam configuration at 26 GHz and 17.6 GHz, employing the optimum QAM order according to Fig. 13.

As depicted in Fig. 11, variable optical attenuators (VOAs) are included before photodetection to evaluate the system performance with the received optical power level (P_{PIN}). Fig. 14 shows the measured EVM for single-carrier 16QAM signals at 26 GHz for different received optical power levels. Fig. 14 compares the performance of 1.5 GHz and 3.25 GHz BW signals operating at λ=1545.185 nm which, according to Table I, provides an increment delay of $\Delta\tau$=13.83 ps that is translated to a beam steering of θ=46°.
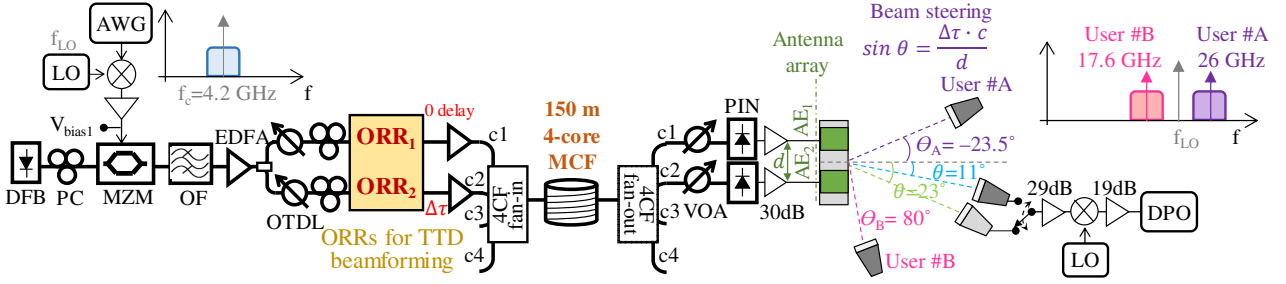
Fig. 11. Experimental setup for 2×1 beamforming system evaluation of optical and wireless performance employing the TTD beamforming chip based on ORRs and MCF to connect the antenna array
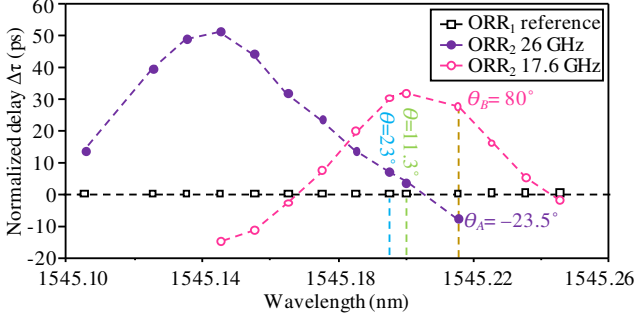

Fig. 12. Normalized delay increments for different wavelengths measured with 26 GHz (user #A) and 17.6 GHz (user #B) considering signal at core 1 (ORR$_1$) as reference. Resulting beam-steering angles included in labels

TABLE III
PROVIDED DATA RATE FOR EACH 5G SIGNAL BANDWIDTH USING THE OPTIMUM MODULATION ORDER IN A 2×1 BEAMFORMING SYSTEM

Electrical bandwidth (BW)	Optimum modulation order	Provided data rate
1.5 GHz	128QAM	10.5 Gbps
2 GHz	128QAM	14 Gbps
3.25 GHz	64QAM	19.5 Gbps
4.2 GHz	32QAM	21 Gbps

It can be observed in Fig. 14(a) that 1.5 GHz BW signals require power levels equal or higher than $P_{PIN} \geq -10$ dBm in order to meet the EVM recommendation. Increasing the BW to 3.25 GHz (BW occupied by the 5G band at 26 GHz) requires $P_{PIN} \geq -8$ dBm, which means that doubling the electrical bandwidth for the same delay configuration requires extra +2 dB received power.

The 2×1 wireless transmission in the 26 GHz band for 5G NR communication is evaluated in a laboratory environment using an array of bow-tie antennas as transmitter with a separation between the two AEs of $d=c/2f=5.75$ mm and a horn antenna as receiver (FM LTD model 22240-20).

As labelled in Fig. 12 and confirmed by the wireless transmission included in Fig. 15, operating at a wavelength of 1545.195 nm the delay increment is $\Delta\tau=7.51$ ps, which for a radio signal at 26 GHz corresponds to a beam steering of 23°. Tuning the DFB laser wavelength to 1545.200 nm, the delay is reduced to $\Delta\tau=3.77$ ps, which changes the steering to 11.3°. Fig. 15 shows the received constellations and measured EVM after wireless transmission for 16QAM signals at 26 GHz.
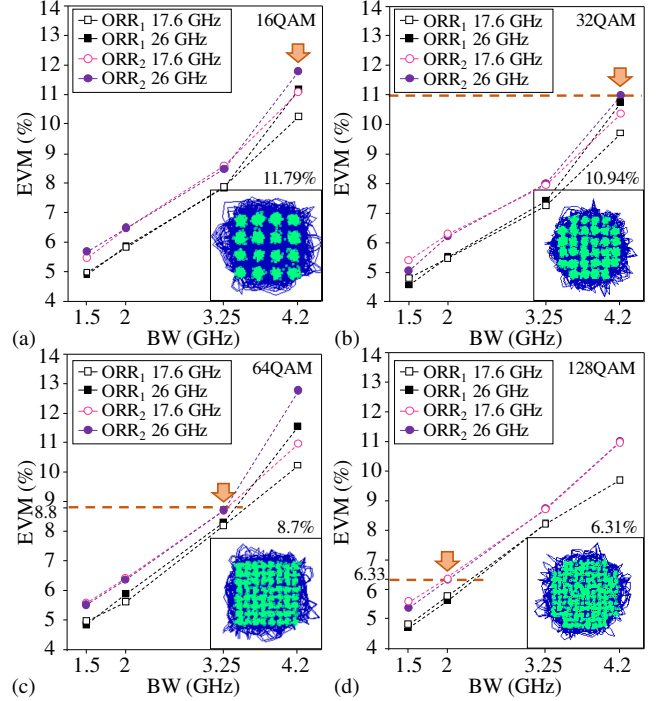

Fig. 13. Measured rms EVM vs. BW for all ORRs in a 2×1 beamforming system at 1545.215 nm providing multiple beams, $\theta_A = -23.5°$ at 26 GHz and $\theta_B = 80°$ at 17.6 GHz using: (a) 16QAM, (b) 32QAM, (c) 64QAM and (d) 128QAM. Inset constellations for each modulation order measured for ORR$_2$ at 26 GHz with the highest BW meeting the recommendation (marked with arrows)
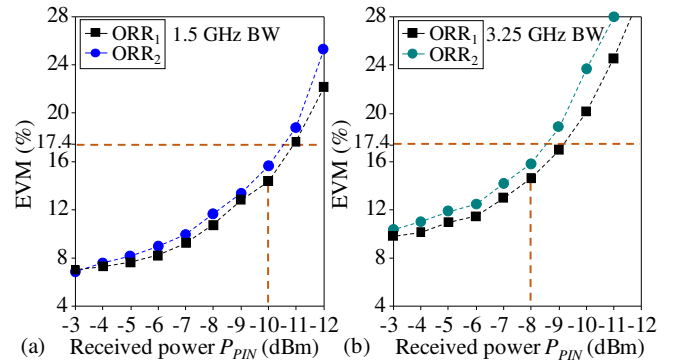

Fig. 14. Measured rms EVM of 26 GHz signals at λ=1545.185 nm (resulting beam steering of $\theta=46°$) vs. received optical power level at the photodiode for: (a) 1.5 GHz and (b) 3.25 GHz BW signals. In both cases, ORR$_1$ is considered the reference delay and ORR$_2$ is configured to be $\Delta\tau=13.83$ ps
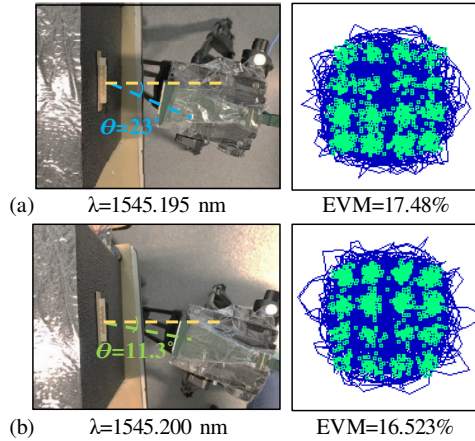
(a) λ=1545.195 nm EVM=17.48%

(b) λ=1545.200 nm EVM=16.523%

Fig. 15. Received constellations after 2×1 wireless transmission at 26 GHz and measured rms EVM for: (a) λ=1545.195 nm with beam steering of θ=23° and (b) λ=1545.200 nm with beam steering of θ=11.3°

IV. CONCLUSION

In this paper, a photonic TTD beamforming system operating in the mm-wave band based on ORRs implemented on Si_3N_4 and controlling the beamformer through MCF is proposed and demonstrated experimentally. With the proposed approach, the most complex functions (including the beamforming network) are implemented at the central office, thus reducing the complexity, cost and power consumption of the remote antenna units. Using MCF to connect all the AEs ensures that all the optical paths have the same length and that the delay increment is induced by the TTD chip. The resulting beam steering can be modified from a central computer by tuning the ORRs' heaters (slow steering) or by changing the operating wavelength of the optical laser (fast steering). With the proper configuration of the ORRs, a delay difference between paths larger than $\Delta\tau > 180$ ps can be obtained.

The photonic beamformer performance with four AEs is evaluated with single-carrier signals in the 26 GHz band proposed for 5G NR operation in Europe. The beamforming performance is evaluated employing 4 ORRs and a 4-core fiber. Up to 16.8 Gbps per user is provided employing 4.2 GHz bandwidth signals in a beamforming system comprising four antenna elements (suitable for 2×2 matrix antennas or 4×1 array antennas) obtaining a 23° beam steering at 26 GHz.

The experimental demonstration also evaluates a complete 2×1 beamforming system. Multi-beam capability is confirmed providing 26 GHz and 17.6 GHz signals simultaneously with 103.5° beam separation with up to 21 Gbps per user. The optical evaluation indicates that to provide 3.25 GHz BW signals requires +2 dB more received optical power compared with 1.5 GHz BW signals. The wireless transmission confirms that tuning the wavelength from 1545.200 to 1545.195 nm modifies the beam steering from 11.3° to 23° with 26 GHz signals. The proposed TTD beamformer enables the centralized configuration of the induced delays and corresponding beam steering with great flexibility, providing high capacity for 5G NR communications.

REFERENCES

[1] 3GPP Release 15, *5G NR specifications*, TR 21.900 V15.1.0 (09-2018).

[2] Huawei Technologies Co., "5G unlocks a world of opportunities: top ten 5G use cases," Huawei Mobile Broadband Insights & Reports [Online], Nov. 2017. Available: https://www.huawei.com/en/industry-insights/outlook/mobile-broadband/insights-reports/5g-unlocks-a-world-of-opportunities

[3] Ofcom, "5G spectrum access at 26 GHz and update on bands above 30 GHz," Ofcom consultations and statements [Online], July 2017. Available: https://www.ofcom.org.uk/consultations-and-statements/category-2/5g-access-at-26-ghz

[4] O. El Ayach, S. Rajagopal, S. Abu-Surra, Z. Pi and R.W. Heath, "Spatially sparse precoding in millimeter wave MIMO Systems," IEEE Trans. Wireless Commun., vol. 13, no. 3, pp. 1499-1513, March 2014.

[5] K. Kibaroglu, M. Sayginer and G. M. Rebeiz, "A low-cost scalable 32-element 28-GHz phased array transceiver for 5G communication links based on a 2×2 beamformer flip-chip unit cell," IEEE J. Solid-State Circuits, vol. 53, no. 5, pp. 1260-1274, May 2018.

[6] M. Burla, et al., "Multiwavelength-integrated optical beamformer based on wavelength division multiplexing for 2-D phased array antennas," IEEE/OSA J. Lightw. Technol., vol. 32, no. 20, pp. 3509-3520, Oct. 2014.

[7] A. Meijerink et al., "Novel ring resonator-based integrated photonic beamformer for broadband phased array receive antennas—Part I: Design and performance analysis," IEEE/OSA J. Lightw. Technol., vol. 28, no. 1, pp. 3-18, Jan. 2010.

[8] C. Masterson, "Massive MIMO and Beamforming: the signal processing behind the 5G buzzwords," Analog Dialogue 51-06, June 2017.

[9] D. C. Beste and E. N. Leith, "An Optical Technique for Simultaneous Beamforming and Cross-Correlation," IEEE Trans. Aerosp. Electron. Syst, vol. AES-2, no. 4, pp. 376-384, July 1966.

[10] G. Grosskopf et al., "Photonic 60-GHz maximum directivity beam former for smart antennas in mobile broad-band communications," IEEE Photon. Technol. Lett., vol. 14, no. 8, pp. 1169-1171, Aug. 2002.

[11] A. P. Goutzoulis, D. K. Davies, and J. M. Zomp, "Hybrid electronic fiber optic wavelength-multiplexed system for true time-delay steering of phased array antennas," Opt. Eng., vol. 31, no. 11, pp. 2312-2322, 1992.

[12] R. Soref, "Optical dispersion technique for time delay beam steering," Appl. Opt., vol. 31, no. 35, pp. 7395-7397, Dec. 1992.

[13] J. L. Corral, J. Marti, J. M. Fuster, and R. I. Laming, "Dispersion-induced bandwidth limitation of variable true time delay lines based on linearly chirped fibre gratings," Electron. Lett., vol. 34, no. 2, pp. 209-211, Jan. 1998.

[14] N. Tessema, et al., "A tunable Si3N4 integrated true time delay circuit for optically-controlled K-band radio beamformer in satellite communication," IEEE/OSA J. Lightw. Technol., vol. 34, no. 20, pp. 4736-4743, Oct. 2016.

[15] W. Roh, et al., "Millimeter-wave beamforming as an enabling technology for 5G cellular communications: Theoretical feasibility and prototype results," IEEE Commun. Mag., vol. 52, no. 2, pp. 106-113, Feb. 2014.

[16] A. Morales, I. Tafur Monroy, F. Nordwall and T. Sørensen, "50 GHz optical true time delay beamforming in hybrid optical/mm-wave access networks with multi-core optical fiber distribution," OSA Chinese Optics Lett., vol. 16, no. 4, pp. 040603, April 2018.

[17] M. Morant, A. Macho and R. Llorente, "On the suitability of multicore fiber for LTE–Advanced MIMO optical fronthaul systems," IEEE/OSA J. Lightw. Technol., vol. 34, no. 2, pp. 676-682, Jan. 2016.

[18] A. Sayeed and J. Brady, "Beamspace MIMO for high-dimensional multiuser communication at millimeter-wave frequencies," 2013 IEEE Global Comm. Conf. (GLOBECOM), Dec. 2013.

[19] C. Tidestav, "Massive beamforming in 5G radio access," Ericsson Research Blog [Online], March 2015. Available: https://www.ericsson.com/research-blog/massive-beamforming-in-5g-radio-access/

[20] Y. Aslan, J. Puskely, J. H. J. Janssen, M. Geurts, A. Roederer and A. Yarovoy, "Thermal-aware synthesis of 5G base station antenna arrays: an overview and a sparsity-based approach," IEEE Access, vol. 6, pp. 58868-58882, Oct. 2018.

[21] L. Aluigi, G. Orecchini and L. Larcher, "A 28 GHz scalable beamforming system for 5G automotive connectivity: an integrated patch antenna and power amplifier solution," 2018 IEEE MTT-S Int.

Microwave Workshop Series on 5G Hardware and System Techn. (IMWS-5G), August 2018.

[22] Ericsson, "SK telecom and Ericsson conduct first multi-vehicular 5G trials with BMW," Ericsson press release [Online], Nov. 2016. Available: https://www.ericsson.com/en/press-releases/2016/11/sk-telecom-and-ericsson-conduct-first-multi-vehicular-5g-trials-with-bmw

[23] M. Alleven, "Japan's DoCoMo claims 5G first in field trial involving 28 GHz and ultrahigh mobility," Fierce wireless [Online], May 2018, Available: https://www.fiercewireless.com/wireless/japan-s-docomo-claims-5g-first-field-trial-involving-28-ghz-and-ultra-high-mobility

[24] A. Weissberger, "NTT DoCoMo achieves 28GHz wireless data transmission in ultrahigh mobility environment," IEEE Communications Society Technology Blog [Online], May 2018. Available: http://techblog.comsoc.org/2018/05/11/ntt-docomo-claims-5g-first-in-field-trial-involving-28-ghz-and-ultrahigh-mobility/

[25] D. Kumar and R. Ranjan, "Estimation of crosstalk in homogeneous multicore fiber for high core count under limited cladding diameter," 2017 Conf. on Information and Comm, Techn, (CICT), Nov. 2017.

[26] K. Takenaga, S. Matsuo, K. Saitoh, T. Morioka, Y. Miyamoto, "High-density multicore fibers," 2016 Optical Fiber Comm. Conf. (OFC), March 2016.

[27] ITU-T Recom. Std. G.975.1, "Forward error correction for high bit-rate DWDM submarine systems," 2004.

Maria Morant (S'07–M'12) received the M.Sc. degree in telecommunication engineering and the International Ph.D. degree from the Universitat Politècnica de València, Valencia, Spain, in 2008 and 2012, respectively. Since 2006, she has been investigating optical techniques for the radio-over-fiber transmission in access networks at Valencia Nanophotonics Technology Center (NTC). She is currently a postdoc researcher at NTC working in advanced optical sensing and next-generation MIMO communications. She has participated in European projects dealing with optical communications and optical sensing such as FP7-ICT-FIVER, FP7-IST-UCELLS and FP6-IST-UROOF and in national projects like ULTRADEF, VISICONEC, XCORE and HIDRASENSE. Her current research interests include advanced modulations and optical sensing techniques.

Ailee Trinidad (S'16) received her master's degree in photonics engineering from Ghent University and Vrije Universiteit Brussel, Belgium. She is currently working as a Ph.D. researcher with the Eindhoven University of Technology in the Netherlands since 2016. Her current research interests include photonic integration, radio over fiber, and millimeter-wave beamforming system design.

Eduward Tangdiongga (S'01–M'10) received the M.Sc. and Ph.D. degrees from the Eindhoven University of Technology, The Netherlands, in 1994 and 2001, respectively. In 2001, he joined COBRA Research Institute working on ultrafast optical signal processing using semiconductor devices. In 2016, he was an Associate Professor on advanced optical access and local area networks. His current research interests include passive optical networks, radio over (single mode-, multimode-, and plastic) fiber, and optical wireless communication.

Ton Koonen (F'07) is a Full Professor in Eindhoven University of Technology since 2001. Since 2004, he has been the Chairman of the Group Electro-Optical Communication Systems and since 2012 the Vice-Dean of the Department of Electrical Engineering. Before 2001, he worked for more than 20 years in applied research in industry, among others in Bell Labs - Lucent Technologies. He is a Bell Labs Fellow (1998), an OSA Fellow (2013), and a Distinguished Guest Professor of Hunan University, Changsha, China, in 2014. In 2011, he received the Advanced Investigator Grant of the European Research Council. His current research interests include spatial division multiplexed systems, access and in-building fiber networks, including high-capacity POF networks, radio-over-fiber techniques and wireless optics techniques.

Roberto Llorente (IEEE M'99, OSA SM'17) is Full Professor in the Universitat Politècnica de València (UPV), Spain. He has been since 2002 with the Valencia Nanophotonics Technology Center (www.ntc.upv.es), a designated singular scientific & technical institution (ICTS) by the Government of Spain, being appointed deputy director in 2015. He has been leading the Optical Networks and Systems research unit in the NTC, being coordinator or principal researcher of several projects in the framework of European Union's Research and Innovation programmes FP6, FP7 and H2020. He has also led more than 50 national-level research and technology-transfer projects bringing together highly specialized companies and academia in Spain. His current research interests include electro-optic processing techniques applied to high-performance applications as 5G fronthaul beamforming, photonic sensing, and secure photonic network architectures.